Forensic Imaging 37 (2024) 200596

Contents lists available at ScienceDirect

Forensic Imaging

journal homepage: www.sciencedirect.com/journal/forensic-imaging

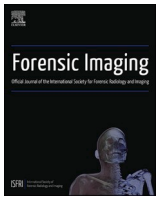

Scaling up contrast-enhanced micro-CT imaging: Optimizing contrast and acquisition for large ex-vivo human samples

Daniël Docter [a,b,c,d], Melanie Timmerman [e], Yousif Dawood [b,c], Jaco Hagoort [f], Nick Lobe [g], Ernst van Heurn [a,c,d], Ramon Gorter [a,c,d], Karl Jacobs [c,f,h], Grzegorz Pyka [i,j], Greet Kerckhofs [i,j,k,l], Maurice J.B. van den Hoff [c,f], Bernadette de Bakker [b,c,m,*]

[a] Department of Pediatric Surgery, Emma Children's Hospital, Amsterdam UMC, location AMC, Meibergdreef 9, 1105 AZ Amsterdam, The Netherlands
[b] Department of Obstetrics and Gynecology, Amsterdam UMC, location AMC, Meibergdreef 9, 1105 AZ Amsterdam, The Netherlands
[c] Amsterdam Reproduction and Development research institute, Meibergdreef 9, 1105 AZ Amsterdam, The Netherlands
[d] Amsterdam Gastroenterology Endocrinology Metabolism, Meibergdreef 9, 1105AZ Amsterdam, The Netherlands
[e] Department of Forensics, GGD Amsterdam, The Netherlands
[f] Department of Medical Biology, Amsterdam UMC location AMC, Meibergdreef 15, 1105AZ Amsterdam, The Netherlands
[g] Department of Radiology, Amsterdam UMC, location AMC, Meibergdreef 9, 1105AZ Amsterdam, The Netherlands
[h] Department of Oral Pain and Dysfunction, Functional Anatomy, Academic Centre for Dentistry Amsterdam (ACTA), University of Amsterdam and VU University Amsterdam, 1081 LA Amsterdam, The Netherlands
[i] Mechatronic, Electrical Energy and Dynamic Systems, Institute of Mechanics, Materials and Civil Engineering, Université catholique de Louvain, Louvain-la-Neuve, Belgium
[j] Pole of Morphology, Institute of Experimental and Clinical Research, Université catholique de Louvain, Brussels, Belgium
[k] Department of Materials Engineering, KU Leuven, Heverlee, Belgium
[l] Prometheus, Division for Skeletal Tissue Engineering, KU Leuven, Leuven, Belgium
[m] Erasmus MC – Sophia Children's Hospital, University Medical Center Rotterdam, Department of Pediatric Surgery, The Netherlands

ARTICLE INFO

Keywords:
Micro-CT
Forensic
Anatomical
Fetal
Contrast enhancement
Methodological
Microscale
B-lugol
Microfocus computed tomography

ABSTRACT

Microfocus Computed Tomography (Micro-CT) is a novel method for non-destructive 3D imaging of samples, reaching microscale resolutions. While initially prominent in material sciences for small samples, micro-CT now gains significance in biological and medical studies. Here we present our utilization of micro-CT for imaging large ex-vivo human samples for anatomical and forensic research in three recent experiments and discuss the fundamentals of micro-CT imaging.

For pelvic anatomical research, whole human pelvises were imaged to explore nerve anatomy around the prostate using various concentrations of buffered lugol (B-lugol). Advanced acquisition protocols were essential due to X-ray attenuation properties of the sample, which required higher energy for sufficient photon transmission.

For fetal research, B-lugol stained fetuses of 20–24 gestational weeks underwent full body imaging. However, this led to challenging acquisition parameters and images of insufficient quality. Subsequent destaining yielded less dense, yet contrast-maintaining samples allowing higher quality images. Refined acquisition protocols with reduced energy improved image quality.

For forensic research, explanted hyoid-larynx complexes were imaged. Micro-CT imaging showed potential in visualizing micro-fractures. The addition of B-lugol allowed for excellent soft tissue contrast and promising possibilities for forensic evaluation.

In conclusion, micro-CT imaging accommodates a diversity of large ex-vivo human samples for anatomical and forensic purposes, though challenges arise with optimal soft tissue staining and acquisition protocols. We describe partial destaining as a new possibility to alleviate scanning issues to improve scan quality and highlight topics for future research. Micro-CT imaging is a promising new avenue for medical research and forensic evaluation.

* Corresponding author.
E-mail address: b.s.debakker@amsterdamumc.nl (B. de Bakker).

https://doi.org/10.1016/j.fri.2024.200596

Available online 27 April 2024

Introduction

Complementary to dissection, computed tomography (CT) has been a widely used imaging technique to study postmortem human anatomy non-invasively, enabling the evaluation of internal structures with impressive detail [1]. Clinical CT imaging however has its limitations, especially when it comes to visualizing microscale anatomical features. To overcome these challenges, advancements in the form of microfocus computed tomography (micro-CT) imaging have emerged as a promising avenue, offering enhanced contrast and spatial resolution for detailed analysis [2]. Micro-CT has revolutionized the field of tomography. It utilizes X-ray technology to provide non-destructive, high--resolution, and three-dimensional imaging of objects in 3D microscale resolution down to 1 micrometer voxel size. A clinical CT scan typically reaches a volume pixel (voxel) size of 500 micrometers [3], whereas micro-CT scanning reaches voxel sizes of a couple of micrometers and can even reach nanometer size in small samples (i.e. <1 cm) [4]. High-resolution visualization of microscale structures enables us to deepen our understanding of the 3D morphology of tissues and to enrich our understanding of the pathologic bases of disease.

Abbreviations

microfocus computed tomography Micro-CT
Sorensen buffered lugol B-lugol
volume pixel Voxel
paraformaldehyde PFA
diffused iodine-base contrast-enhanced computed tomography dice-CT
hyoid-larynx complex HLC
Robot Assisted Laparoscopic Prostatectomy RALP
Signal-to-noise ratio SNR
Mean grey value MGV
computed tomography CT

Micro-CT imaging has been tested in various disciplines of forensic evaluation such as analyses of pediatric rib fractures in suspected child abuse cases [5] or hairline fractures in the hyoid-larynx complex (HLC) in strangulation cases of advanced decomposed bodies [6]. Moreover, micro-CT has been used to investigate the impact of gunshots on fabric, tissue and bone [7], to evaluate tool marks in forensic cases [8,9] or to estimate postmortem intervals [10,11]. While micro-CT has proven effective for anatomical and forensic studies with small samples [12–15], we found in our experiments that it faces challenges when dealing with larger ex-vivo human specimens such as the adult pelvic area or fetuses with a gestational age above 20 weeks. Biological samples suitable for micro-CT are typically a couple of mm or cm large, exceptions being an entire rat [16] or an entire adult human heart [17].

In this study we explored the possibility to image human hyoid larynx complexes of approximately 5 cm, fetuses up to a crown rump length of 25 cm and whole pelvic sample of 30 × 30 cm, weighing over 1200 g. In these large samples, tissue composition is complex and each additional tissue layer increase the overall density of the sample. This high density makes acquiring sufficient X-ray transmission challenging. As a consequence, scanning these tissues requires increased energy levels of the X-ray beam and longer acquisition times (of up to several hours). The latter can lead to motion artifacts and as a result in images of lesser quality. Additionally, the contrast enhancement in these large specimens becomes challenging due to increased X-ray attenuation and scattering. Moreover, large differences in tissue density in an individual sample can compromise scan quality as less dense parts of the sample suffer more from higher energy required to penetrate the denser parts. As a result, the visualization of fine structures within large specimens can be compromised, limiting the full potential of micro-CT imaging in these cases.

The aim of this manuscript is to share our experience with contrast-enhanced Micro-CT imaging of three types of large human samples. To the best of our knowledge, these are some of the largest biological samples that have ever been imaged using micro-CT imaging. These challenging samples called for advanced acquisition protocols. By building upon existing micro-CT advancements, we describe here how we dealt with these challenges and how they can be overcome in future research. By optimizing micro-CT imaging techniques for larger samples, we aspire to expand the horizons of anatomical research and the clinical practice of postmortem scanning, unveiling the microscopic realm with unprecedented clarity and detail as a new research and possibly diagnostic method for forensic evaluation.

Materials and methods - results

Specimens for anatomical research

Adult human specimens were obtained from cadavers donated to the Department of Medical Biology, section Clinical Anatomy & Embryology, Amsterdam University Medical Centers (Amsterdam UMC), location AMC, Amsterdam the Netherlands. People can chose by life if they wish to donate their remains for scientific research and education by providing a handwritten consent form to the department in accordance with Dutch law and legislation. When the remains are brought to this institution, they are fixed with embalming solution containing 4 % formalin by endovascular administration. Perfusion is continued until peripheral vessels appear to contain the embalming fluid. Finally, the cadavers are stored in embalming storage solution for 3 months at 4 °C for optimal fixation.

Specimens for fetal research

All fetal samples were derived from the Dutch Fetal Biobank in Amsterdam UMC [18], the Netherlands. Ethical approval was acquired through the accredited Medical Research Ethics Committee Amsterdam UMC (METC2016_285) and all practices are in accordance with the Dutch law and legislation. Anonymously donated complete fetuses are fixed by submersion in 4 % paraformaldehyde (PFA) freshly dissolved in PBS (10 mM NaH2PO4/Na2HPO4 and 150 mM NaCl) within 6 hours after delivery for a total of 2-7 days. After fixation they are stored in 0.2 % PFA-PBS until they are requested and approved for research.

Specimens for forensic research

Twenty hyoid-larynx complexes (HLC), including five pediatric samples, were obtained from forensic autopsies of the department of Forensic Medicine of the Antwerp University Hospital, Belgium. The Ethics Review Board of Antwerp University Hospital approved this study protocol on April 25, 2022 (Project ID 3222 – Edge n/a - BUN B3002022000048). Samples were excised during routine forensic pathologic evaluation. Samples were immediately fixed and stored in 4% formalin for a minimum of 7 days for optimal fixation.

Sample staining

In these studies, we intended to investigate soft tissue within these specimens. To gain soft tissue contrast, a staining agent had to be utilized. This was accomplished by using an iodine substance, commonly referred to as diffused iodine-base contrast-enhanced computed tomography (dice-CT) [19]. Here we utilized 3.75 % B-Lugol, a buffered version of Lugol's iodine (2.5 % w/v KI and 1.25 % w/v I2) which has excellent staining properties for soft tissue and the addition of Sörensen buffer (133 mM Na2HPO4/KH2PO4 pH7.2) which diminishes and even

prevents tissue shrinkage, which is frequently observed using non-buffered Lugol's solution [20]. Samples are submerged in 20x the volume of the sample and staining was monitored using medical CT scanning. All solutions have been tested and monitored for concentration and pH levels and refreshed if necessary. When staining was complete, which could take several weeks or months, the samples were incubated for 24 h in PBS to remove excess Lugol prior to scanning on a micro-CT scanner as specified above.

CT acquisition and data extraction

To monitor staining progression prior to micro-CT scanning, samples were scanned using a third generation dual source Somatom Force scanner (Siemens Healthineers, Erlangen, Germany) available through the Department of Radiology, Amsterdam UMC. Unstained forensic samples were scanned using a Phoenix Nanotom M (GE Sensing & Inspection Technologies GmbH, Germany). B-lugol stained (more dense) material was scanned using a UniTOM XL Micro-CT (TESCAN, Brno, Czech Republic). This micro-CT scanner is equipped with a higher-powered radiation source. Micro-CT scanners were available through the Department of Material Sciences, KU Leuven and reconstructed using recommended reconstruction software of the developer of the respective scanners. All data was accessed and viewed with Amira software version 2022.1 licensed to the Department of Medical Biology, Amsterdam UMC.

Experiment one: studying surgical anatomy of the pelvic region

Background

After prostatectomy using Robot Assisted Laparoscopic Prostatectomy (RALP), patients are often left with complications such as incontinence and impotence [21]. The purpose of this research was to investigate structures surrounding the prostate and in the retro pubic space that may contribute to continence, particularly the branches of the Inferior Hypogastric Plexus (IHP) [22,23]. To retain the topographical relations of this structure, we sought to image soft tissue, while inside the pelvis, in a resolution that enabled us to differentiate the terminal branches. This was a pilot study to test dissection, staining, and acquisition protocols and to update these after preliminary results.

Methods and results

The lower half of the torso of a formalin-fixed cadaver was isolated and the extremities removed. It was then dissected to increase surface area and reduce mass to enhance contrast uptake. After dissection the pelvic bone was laid bare and the ischiorectal space was cleared of fat to reveal the pelvic floor muscles. These were left untouched as well as the genitalia. After dissection, the specimen weight was 1200 g. Because of the size of the specimen, it was submerged in 25 liters of 7.5 % B-lugol. We used 7.5 % in contrast to the normally used 3.75 % B-Lugol in an attempt to speed up the staining progress. Evaluating the staining process using a clinical CT scanner, it was thought that the specimen had sufficient contrast after 35 days of staining (Fig. 1). It was mounted in plastic containers and stabilized using Styrofoam cutouts. However, the subsequent micro-CT data revealed that the contrast was still lacking in the central part of the specimen. This finding indicated that insufficient staining agent had reached the center of the sample (Fig. 2). The specimen was again submerged in fresh B-lugol solution and follow up scans were made (Fig. 1). After 3 months of staining, more contrast could reach the center of the sample. However, due to the longevity of the staining procedure, other smaller samples of the pelvic area were made to decrease the staining time and speedup this anatomical research (Fig. 2).

Experiment two: large fetal samples

Background

To gain new insights in human development, human embryos and fetuses are frequently studied by this research group using micro-CT imaging. The images are used to create open source 3D datasets of different stages of fetal and embryological development for research and educational purposes [13]. Here we present the challenges we faced with imaging large fetal specimens of 20-24 weeks gestation using micro-CT.

Method and results

Four complete healthy fetal specimens of 20-24 weeks gestational age were acquired through the *Dutch Fetal Biobank [18]*. Submerged in 3.75 % B-lugol for 4-6 weeks and scanned using clinical CT to monitor stain progression. When samples were adequately stained on clinical CT, indicated by soft tissue contrast in the center of the sample and even density values in similar structures throughout the sample, they were

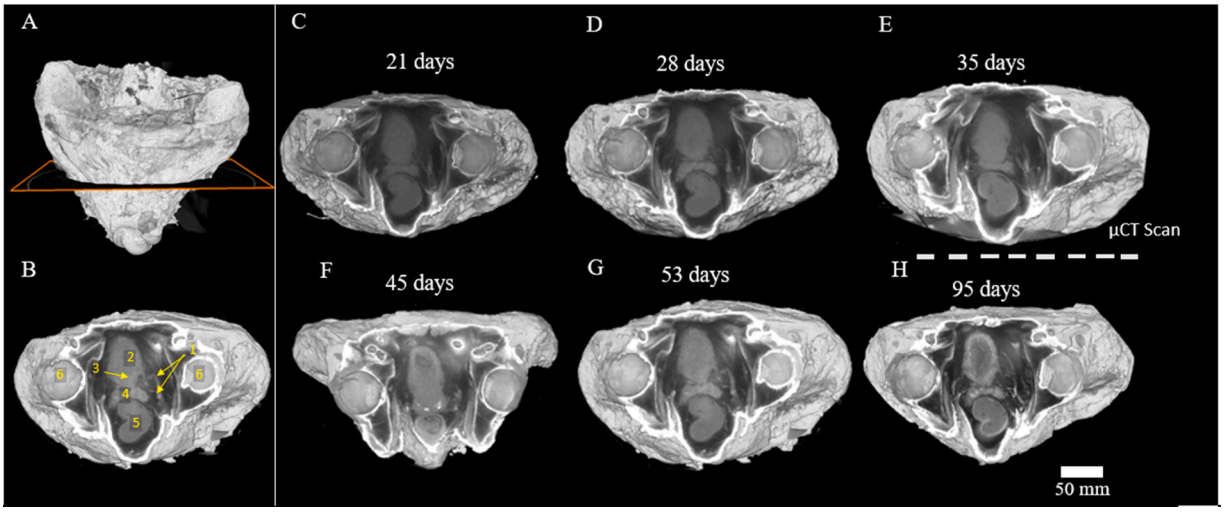

Fig. 1. Iodine uptake over time in pelvic specimen stained using 7,5 % B-Lugol. 3D reconstruction of clinical CT scan. **1.A** Ventral view of a 3D volume rendering of the specimen with marking of the transversal section used in other planes. **1.B** Anatomically marked version of slice. **1.C** 21 days of staining **1.D** 28 days of staining **1.E** 35 days of staining, μCT scan was made after this medical CT scan. **1.F** 45 days of staining, due to partial collapse during scan, figure looks slightly different compared to others. **1.G** 53 days of staining. **1.H** 95 days of staining.
Legend: 1. Lateral structures (increasingly visible with prolonged staining) 2. Urinary Bladder 3. Bulge of prostate. 4. Seminal Vesicles. 5. Rectum 6. Acetabulum.

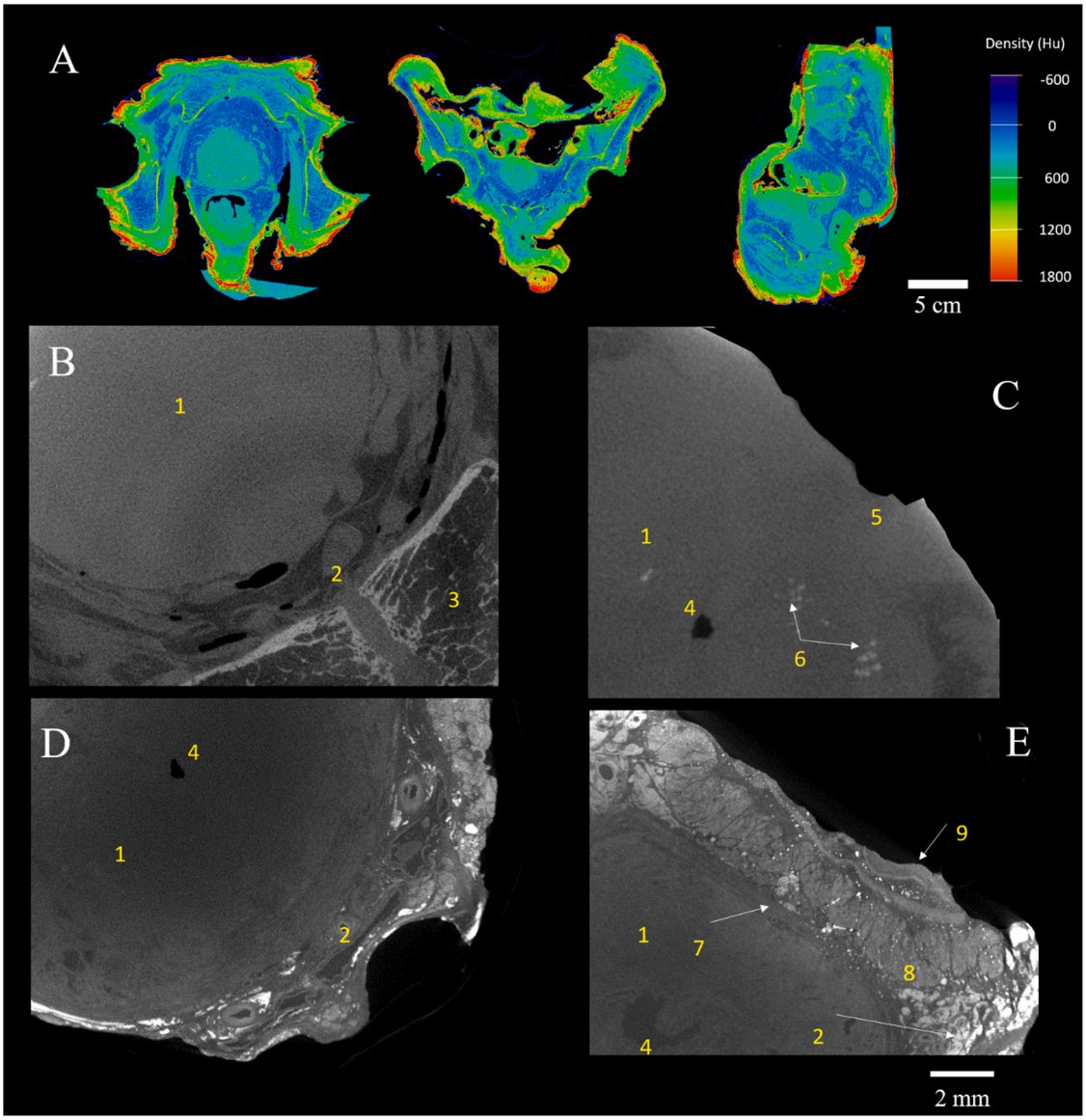

Fig. 2. CT images of Pelvic samples. **2.A** Transverse, coronal and sagittal slices through a medical CT scan after 35 days of staining with density measurements showing that the iodine has penetrated the center of the sample. Small vessels are visible around the prostate giving the appearance of a well-stained sample. **2.B** Micro-CT scan of the same pelvic sample. Transversal slice showing the anterior peri-prostatic space. Contrast is lacking. Small vessels are noticeable but vasculature and innervation are not distinguishable. **2.C** Same scan as 2.B showing the dorsal part of the prostate. Visually no contrast between prostate and rectum is present. **2.D** Micro-CT scan of follow-up experiment where the pelvic contents were excised from the bone and stained for 2 weeks showing major changes in contrast. The center of the sample is still darker, indicating the staining has not fully stained the sample yet. Slice corresponding with 2.B. **2.E** Same scan as 2.D and corresponding to 2.C. Different layers of fascia around the prostate can be identified as well as neurovasculature and layers of the rectum.
Legend: 1. Prostate 2. Neurovasculature 3. Pubic bone 4. Urethra. 5. Undefined rectal wall. 6. Calcifications in the prostate. 7. Prostatic fascia and Denonvilliers' fascia. 8. Muscle 9. Epithelium of rectum.

rinsed in PBS to remove excess B-Lugol. Subsequently they were mounted in containers filled with 1 % agarose gel to prevent movement during scanning and protect them during transport to the scanning facility where the scans were performed the following day. Thin plastic containers or styrofoam boxes where used that closely fitted the samples.

The first scans of these fetal samples resulted in noisy images of insufficient quality (Fig. 3). The samples were demounted and stored in 0.2 % PFA for 4 months. When called upon for additional micro-CT scanning with an updated acquisition protocol, all samples were scanned on the medical CT to re-evaluate the staining. This analysis showed good contrast which was observed throughout the specimen, yet the density of the sample had decreased. The samples were remounted and scanned on the micro-CT using adapted, more favorable, acquisition parameters. This resulted in images of higher quality (Fig. 3).

To compare image quality, a signal-to-noise ratio (SNR) was calculated for both fetal scans in the most homogenous part of the fetus, in this case the liver. The same area of the liver was chosen in both scans for comparability. Both scans were standardized to the Hounsfield scale. Air was set as a grey value of -1000 and agarose as 0, as this is 99 % water and has the same density. As a value for staining the mean grey value (MGV) per voxel of the segmented liver was calculated and considered a measure of signal. The deviation of this value was seen as noise. The signal to noise ratio was calculated by dividing the MGV by the Noise (Table 1).

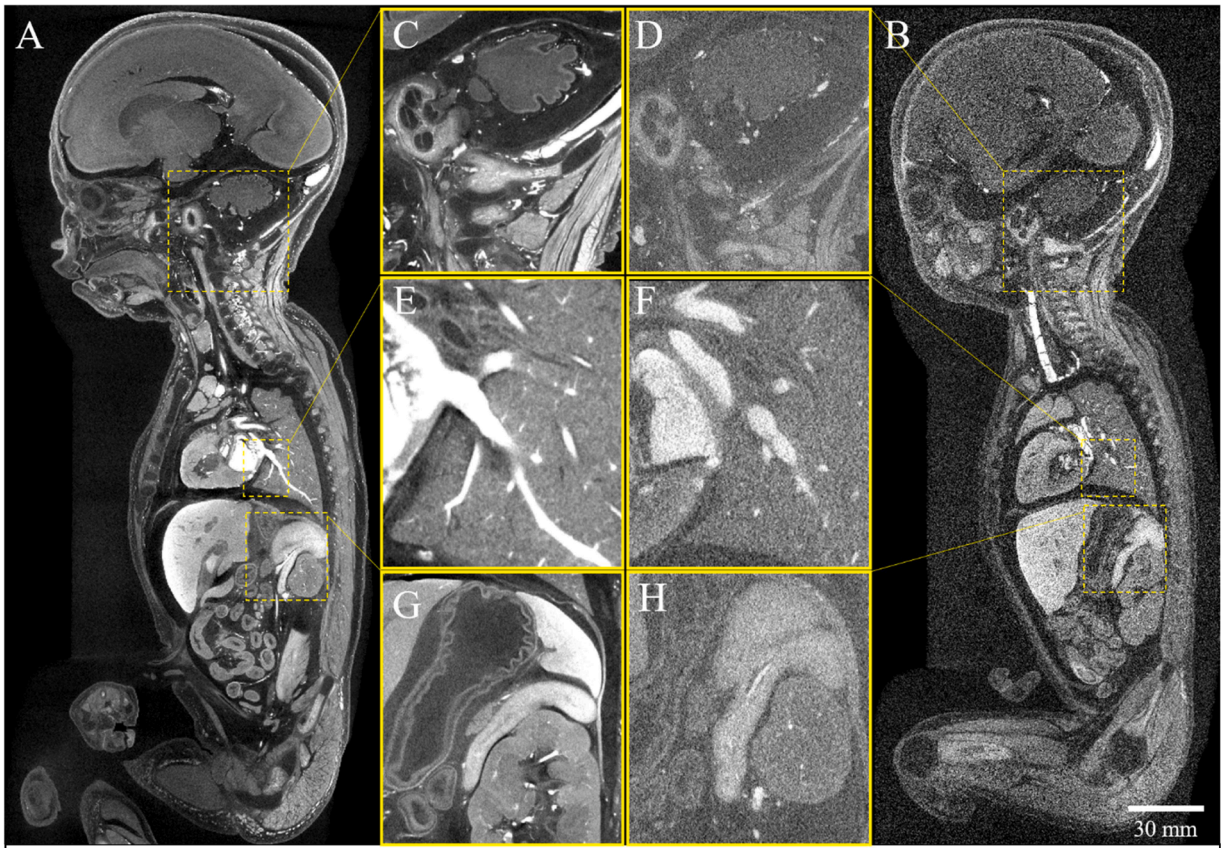

Fig. 3. Fetus of 23 + 4 weeks of gestation scanned under different circumstances.
3.A Midsagittal slice of fetus after 4 months of destaining. **3.B** Midsagittal slice of fetus in initial scan. **3.C** Zoomed in section showing the cerebellum, cochlea and neck musculature **3.D** Slice corresponding with 3.C **3.E** Zoomed in section showing the lung, part of the heart and vasculature **3.F** Slice corresponding with 3.E. **3.G** Zoomed in section showing the stomach and kidney **3.H** slice corresponding with 3.G. Notice the difference in noise levels in both scans. The contrast in the second scan (A, C, E,G) is adequate even though the sample was destained for several months. Note that the first scan (B, D, F, H) had a high kV which could increase the noise, which could have been lowered with a longer exposure time if no averaging was performed.

Table 1
Signal to noise ratios.
Comparison of a segmented area of the fetal liver in the first and second micro-CT scan.

Subject	Mean grey value (MGV)	Deviation (Noise)	S/N*
Fetal liver scan 1	1039	114	9.1
Fetal liver scan 2	1151	93	12.3

*S/N ratio is calculated by dividing the signal (MGV) by the noise. A lower signal or higher noise will result in a lower S/N. The higher S/N found in the destained scan supports the higher quality of the image.

Experiment three: hyoid-larynx complexes

Background

Forensic examination of the hyoid-larynx complex (HLC) is crucial in diagnosing (inflicted) neck trauma [24,25]. However, clinical total-body CT scans of a yet non-calcified pediatric HLC lack sensitivity for fracture detection [26,27]. A gas bubble sign can be an indicator for a fracture of the HLC on the clinical CT scanner, which has a sensitivity of 79,2 % [28]. This sensitivity, however, could be even less for micro-fractures as there has been little research done on this subject. The goal of this research was to investigate the utilization of micro-CT in imaging the HLC and in detecting subtle fractures in forensic cases that could have been missed in routine examination. Moreover, we aimed to test B-lugol staining additionally to micro-CT scanning. The high affinity of B-lugol to blood could aid in the detection of hemorrhages in the soft tissues. This could be promising to discriminate between ante- and postmortem fractures of the HLC, as hemorrhages do not appear in postmortem injuries [29].

Methods and results

Twenty excised formalin-fixed HLCs of which five were pediatric and 15 derived from adults were scanned using the Phoenix Nanotom M (GE Sensing & Inspection Technologies GmbH, Germany). Sample weight between 44–178 g depending on size and attached soft tissue such as musculature or the thyroid gland. No addition dissection was performed to minimize the risk of iatrogenic fractures. All samples were scanned prior to B-Lugol staining to identify bone structures and to obtain an overview of the sample (Fig. 4). This resulted in images on which details within the bone could be identified, allowing for the detection of possible micro-fractures (Fig. 4).

Subsequently, the samples were stained with B-Lugol for 4 to 49 days, depending on sample weight. This produced adequately stained samples and revealed excellent soft tissue contrast (Fig. 4). This allowed for analysis of the fractures and soft tissue with utmost quality.

Discussion

To image large ex-vivo human samples using micro-CT imaging for anatomical or forensic purposes, one must overcome staining difficulties and take into account different acquisition parameters. Micro-CT offers a method to image structures of ex-vivo human tissues at a micrometer scale in 3D in a non-destructive fashion (Figs. 2–4). It provides high quality data sets that can be used for educational purposes and as evidence in court, without the need of showing explicit pictures. Moreover,

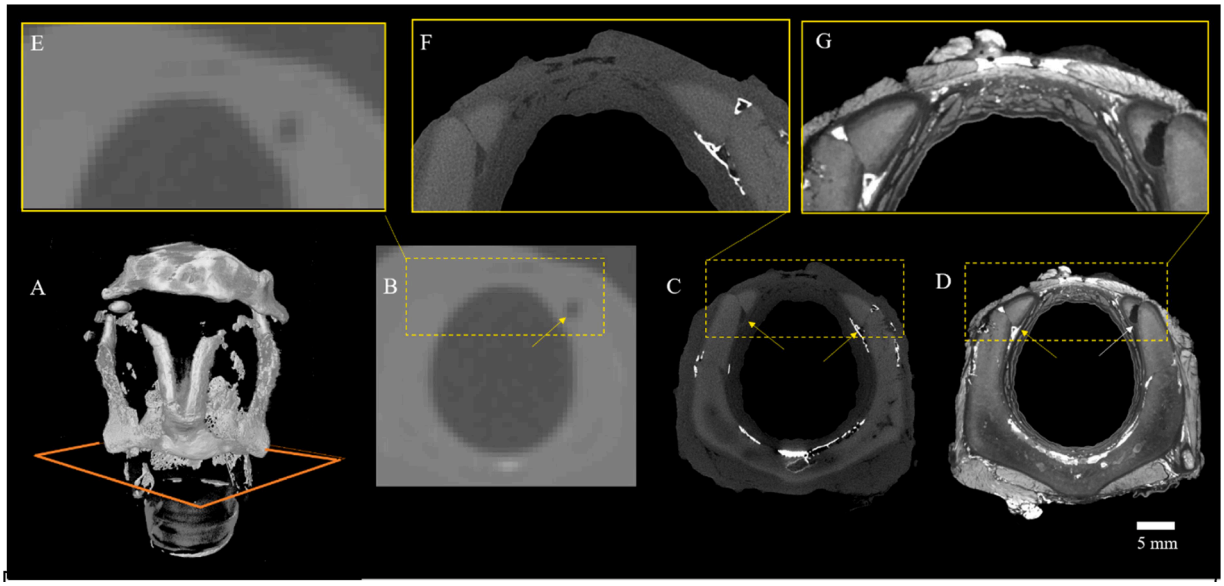

Fig. 4. Evaluation of cricoid cartilage fractures after trauma using different modalities. **4.A** 3D reconstruction of the unstained micro-CT scan. Plane marks the location of other panels **4.B** Axial section of TBCT at cricoid level. Differentiating the structure and assessing possible damage is difficult. Left side of the cricoid shows a small gas bubble sign (arrow), possibly indicating a fracture. **4.C** Unstained micro-CT scan of the same sample. Three possible fractures can be identified (Arrows) **4.D** Stained scan. **4.E** Zoomed in section of 4.B. **4.F** Zoomed in section of 4.C **4.G** Zoomed in section of 4.D.
One fracture line shows hyperdensities indicating blood in the fracture (yellow arrow) and the other does not (white arrow). No blood in the fracture line could indicate that the fracture occurred postmortem. This could help differentiate between ante- and postmortem trauma.

as micro-CT is a non-destructive method, the samples can be further investigated by a pathologist [2]. Classic dissection or histologic evaluation expends the sample. Although not suitable for in vivo practice, this technique promises to be instrumental for postmortem imaging in research setting or for forensic evaluation [12]. These experiments show that scanning large human tissue samples using micro-CT presents new possibilities but also new challenges, which we will discuss.

Staining of soft tissue

Complete staining by submersion in B-lugol is time consuming, because the time to completely stain a sample is dependent on the staining agents speed of diffusion into the tissue and on the distance between the surface and center of the sample [30]. Theoretically, staining speed can be increased with higher concentrations of the staining agent or by increasing the temperature during staining. To date, no research has been undertaken to assess the speed of diffusion using B-lugol. Higher temperatures over extended durations could potentially compromise the integrity of the specimen or cause decompensation. Using a higher B-lugol concentration, 7.5 % rather than 3.75 % B-Lugol, did not have the desired effect on the staining speed in our studies but alternative stain parameters should be the topic of future investigations. An alternative approach could involve postmortem intravascular introduction of the staining agent, such as in postmortem CT-angiography (31). However, this requires an intact vascular system and current micro-CT systems are not yet suited to contain a whole human cadaver. Using the vascular system as a medium to administer the staining agent increases the surface area dramatically. The agent would reach the center more easily and as such it would be worthwhile to explore the application of the staining agent through the vascular system in future research (2). Increasing the tissue surface area and decreasing the distance between the surface and center of the sample by dissection can also increase stain speed. However, anatomical landmarks need to be secured in the sample to allow proper interpretation of the scans.

Destaining tissue

An issue that was encountered in scanning large fetal samples was the high overall density. We observed that large fetal samples that, after staining and initial scanning were stored in 0.2 % PFA for 2-4 months, showed improved contrast and image quality when rescanned (Fig. 3). The overall density of the image decreased, allowing for more favorable scan settings, as discussed in the following paragraph, but the contrast remained in the soft tissue. The chemical properties of B-lugol and the exact mechanisms that are at play while staining samples are unclear. During the process of staining, the triiodide (I3-) diffuses the tissue and selectively binds to distinct molecules which vary between different tissue types. As a consequence of these difference in binding to different tissue, different density levels and X-ray attenuation are observed. Iodide molecules that fail to bind or weakly bind remain in the specimen during superficial rinsing and result in higher overall density. Prolonged incubation in a buffer without the staining agent allow the non and non-specifically bound iodine ions to diffuse out of the tissue more efficiently than specifically bound ions. This results in an improved contrast but with overall less density of the sample. This effect of destaining on tissue samples provides an interesting avenue to explore and in future research the relation between staining and destaining in different size samples needs to be further explored.

Acquisition settings

To produce scans of good quality, certain aspects and parameters need to be considered. First off, adequate X-ray transmission through the sample is required. Transmission is defined as the ratio of photons emitted by a radiation source that reach the detector. A certain number of photons needs to reach the detector, referred to as signal, to produce an image. In our earlier experiments we aspired a transmission of 15–20 % and this percentage can highly differ between micro-CT systems, type of tissue and the overall acquisition protocols. The photons emitted have an energy (kV) value which comprises of a spectrum of higher and lower energy. As sample size and overall sample density increases, more lower energy photons are absorbed in their path by the sample, reducing

transmission and causing a low signal and even scan artefacts. Parameters can be altered to compensate for this such as higher energy, longer exposure times and increased current, leading to more photons.

However, increasing the energy level is limited as high energy photons have the tendency to interact with an atom and yielding only part of their energy to then deviate from their path. This creates a non-information-bearing photon which interferes with other components of the X-ray beam. This is known as the Compton effect [32] which in a reconstructed scan can be observed as noise. Because photons are emitted in a spectrum of energy, some form of this effect is unavoidable, but it can be minimalized. Lower energy values can limit this effect and could have a positive influence on scan quality.

Other ways to increase signal on the detector are tweaking the current and exposure time. Higher currents (mA) provide a larger number of photons and do not decrease image quality. Unfortunately, a higher current increases the spot size, which is the point of the radiation source from which the photons originate. The spot size should be smaller than the voxel size to produce a sharp image. The current should, therefore, be set such that it matches the desired voxel size. When evaluating large specimens (>20 cm) the aspired voxel size is typically larger than in small samples (1 to 3 cm), and as such allows a higher current. The maximal voxel size can be calculated depending on the number of pixels of the detector and the width of the sample. For example, if the detector has 3000 pixels and the sample is 200 mm wide, the maximum voxel that one can achieve is 66 micrometers whereas a 20 mm sample this would be 6 micrometer for a single scan. This of course depends on the scanner and its detector. Another way to increase transmission is by increasing the exposure time. This is the time the detector uses to collect photons. Although this often has a good effect on scan quality due to an increase in the signal to noise ratio, it inevitably leads to longer scan times which is less desirable in a clinical setting or in case of research with limited funding or availability of a scanner. One should take note that increasing these parameters requires a heavy system load and can cause the detector to be oversaturated if the sample is not in the field of view, which leads to damage to the detector and should be prevented.

In our experience with scanning smaller stained samples, lower energy (approx. 80 kV) results in images with the best quality. We also found that lower transmissions (5–10 %) produce surprisingly high-quality images in B-lugol stained specimens. To determine if sufficient transmission is present, one would normally look at the transmission through the densest part of a sample to make sure that even that part is imaged adequately. This is usually the liver in B-lugol stained fetuses. By optimizing the scan for the densest part, less dense structures are neglected and suffer from an increased Compton effect, making the image noisy. By balancing the settings between hyperdense (bones and liver) and hypodense parts of the sample (lungs or intestines), we were able to record images of a high quality with as low as 5 % transmission in the densest parts of our sample. Accepting these low transmission values in relation to optimized current and exposure times, large B-lugol stained specimens still require high energy levels to generate enough transmission, typically between 120–160 kV but sometimes even over 200 kV.

Conclusion

In conclusion, we describe the challenges and solutions in imaging larger human specimens for anatomical or forensic research using micro-CT imaging. The best micro-CT imaging results are always obtained with the smallest samples. Therefore, prior to staining and scanning one should attempt to minimalize the amount of tissue that one desires to investigate, or at least increase the surface area through dedicated dissection. With larger samples one should expect longer staining times and compromised acquisition protocols. Promising alternatives like endovascular admission of stain agents and optimized destaining protocols might help overcome these hurdles and should be investigated in the future. With improved protocols and experience, micro-CT can become a valuable tool for postmortem research and in forensic practice.

Funding

This work was supported by the Amsterdam Reproduction and Development institute with the Grant for Team Science.

CRediT authorship contribution statement

Daniël Docter: Writing – original draft, Visualization, Validation, Methodology, Investigation, Formal analysis, Data curation, Conceptualization. **Melanie Timmerman:** . **Yousif Dawood:** Writing – review & editing, Methodology, Conceptualization. **Jaco Hagoort:** Writing – review & editing, Visualization, Software, Formal analysis. **Nick Lobe:** Writing – review & editing, Investigation. **Ernst van Heurn:** Writing – review & editing, Supervision. **Ramon Gorter:** Writing – review & editing, Supervision, Funding acquisition. **Karl Jacobs:** Writing – review & editing. **Grzegorz Pyka:** Writing – review & editing, Validation. **Greet Kerckhofs:** . **Maurice J.B. van den Hoff:** Writing – review & editing, Methodology. **Bernadette de Bakker:** Writing – review & editing, Supervision, Funding acquisition, Conceptualization.

Declaration of competing interest

The authors declare that they have no known competing financial interests or personal relationships that could have appeared to influence the work reported in this paper.

Acknowledgements

The authors would like to thank the technical staff of the anatomy department of Amsterdam UMC for providing samples and aiding with the dissections. Moreover, we are grateful for the department of Forensic Medicine of the Antwerp University Hospital for providing the forensic samples used in these studies. Lastly, we thank parents for their anonymous donations to the Dutch Fetal Biobank that helped to facilitate this research.

References

[1] G. Ampanozi, Y.A. Thali, W. Schweitzer, G.M. Hatch, L.C. Ebert, M.J. Thali, TD. Ruder, Accuracy of non-contrast PMCT for determining cause of death, Forensic Sci. Med. Pathol. 13 (3) (2017) 284–292.
[2] D. Docter, Y. Dawood, K. Jacobs, J. Hagoort, R.J. Oostra, M.J.B. van den Hoff, et al., Microfocus computed tomography for fetal postmortem imaging: an overview, Pediatr. Radiol. 53 (4) (2023) 632–639.
[3] E. Lin, A. Alessio, What are the basic concepts of temporal, contrast, and spatial resolution in cardiac CT? J. Cardiovasc. Comput. Tomogr. 3 (6) (2009) 403–408.
[4] D.V. Shepherd, J.H. Shepherd, S.M. Best, RE. Cameron, 3D imaging of cells in scaffolds: direct labelling for micro CT, J. Mater. Sci. Mater. Med. 29 (2018) 1–4.
[5] W. Baier, D.G. Norman, MA. Williams, Micro-CT for the examination of paediatric rib injuries: a case series, Forensic Sci. Int. 325 (2021) 110789.
[6] M. Kettner, S. Potente, B. Schulz, P. Knauff, P.H. Schmidt, F. Ramsthaler, Analysis of laryngeal fractures in decomposed bodies using microfocus computed tomography (mfCT), Forensic Sci. Med. Pathol. 10 (4) (2014) 607–612.
[7] J. Newton, A. Savage, N. Coupar, J. Fraser, Preliminary investigation into the use of Micro-CT scanning on impact damage to fabric, tissue and bone caused by both round and flat nosed bullets, Sci. Justice 60 (2) (2020) 151–159.
[8] M.J. Thali, U. Taubenreuther, M. Karolczak, M. Braun, W. Brueschweiler, W. A. Kalender, R. Dirnhofer, Forensic microradiology: micro-computed tomography (Micro-CT) and analysis of patterned injuries inside of bone, J. Forensic Sci. 48 (6) (2003) 1336–1342.
[9] W. Baier, M.J. Donnelly, M. Payne, MA. Williams, A holistic multi-scale approach to using 3D scanning technology in accident reconstruction, J. Forensic Sci. 65 (5) (2020) 1774–1778.
[10] S. Longato, C. Wöss, P. Hatzer-Grubwieser, C. Bauer, W. Parson, S.H. Unterberger, et al., Post-mortem interval estimation of human skeletal remains by micro-computed tomography, mid-infrared microscopic imaging and energy dispersive X-ray mapping, Anal. Methods 7 (7) (2015) 2917–2927.
[11] E. Le Garff, V. Mesli, E. Marchand, H. Behal, X. Demondion, A. Becart, V. Hedouin, Is bone analysis with μCT useful for short postmortem interval estimation? Int. J. Legal. Med. 132 (1) (2018) 269–277.

[12] G.N. Rutty, A. Brough, M.J.P. Biggs, C. Robinson, S.D.A. Lawes, S.V. Hainsworth, The role of micro-computed tomography in forensic investigations, Forensic Sci. Int. 225 (1) (2013) 60–66.
[13] Y. Dawood, M.F.J. Buijtendijk, H. Shah, J.A. Smit, K. Jacobs, J. Hagoort, et al., Imaging fetal anatomy, Semin. Cell Dev. Biol. 131 (2022) 78–92.
[14] J.C. Hutchinson, S.C. Shelmerdine, I.C. Simcock, N.J. Sebire, O.J. Arthurs, Early clinical applications for imaging at microscopic detail: microfocus computed tomography (micro-CT), Br. J. Radiol. 90 (1075) (2017) 20170113.
[15] G. Franchetti, G. Viel, P. Fais, G. Fichera, D. Cecchin, G. Cecchetto, C. Giraudo, Forensic applications of micro-computed tomography: a systematic review, Clin. Transl. ImAging 10 (2022).
[16] E. Tekus, A. Miko, N. Furedi, I. Rostas, J. Tenk, T. Kiss, et al., Body fat of rats of different age groups and nutritional states: assessment by micro-CT and skinfold thickness, J. Appl. Physiol. 124 (2) (1985) 268–275, 2018.
[17] N. Pallares Lupon, J. Duchâteau, L. Yessad, M. Constantin, G. Ramlugun, D. Gerneke, et al., Optimising micro computed tomography imaging of large animal and human hearts at high resolution, Arch. Cardiovasc. Dis. Supplem. 12 (2) (2020) 268–269.
[18] Y. Dawood, M.F.J. Buijtendijk, D. Bohly, Q.D. Gunst, D. Docter, E. Pajkrt, et al., Human embryonic and fetal biobanking: Establishing the Dutch Fetal Biobank and a framework for standardization, Dev. Cell. 58 (24) (2023) 2826–2835.
[19] P.M. Gignac, N.J. Kley, J.A. Clarke, M.W. Colbert, A.C. Morhardt, D. Cerio, et al., Diffusible iodine-based contrast-enhanced computed tomography (diceCT): an emerging tool for rapid, high-resolution, 3-D imaging of metazoan soft tissues, J. Anat. 228 (6) (2016) 889–909.
[20] Y. Dawood, J. Hagoort, B.A. Siadari, J.M. Ruijter, Q.D. Gunst, N.H.J. Lobe, et al., Reducing soft-tissue shrinkage artefacts caused by staining with Lugol's solution, Sci. Rep. 11 (1) (2021) 19781.
[21] V. Trofimenko, J.B. Myers, WO. Brant, Post-prostatectomy incontinence: how common and bothersome is it really? Sex. Med. Rev. 5 (4) (2017) 536–543.
[22] K. Hikita, M. Honda, R. Shimizu, R. Nishikawa, S. Teraoka, Y. Kimura, et al., Advanced reconstruction of vesicourethral support may improve urinary continence and quality of life after non-nerve-sparing robot-assisted radical prostatectomy, In. Vivo (Brooklyn) 37 (1) (2023) 371–377.
[23] V.G. Wagaskar, A. Mittal, S. Sobotka, P. Ratnani, A. Lantz, U.G. Falagario, et al., Hood technique for robotic radical prostatectomy-preserving periurethral anatomical structures in the space of retzius and sparing the pouch of douglas, enabling early return of continence without compromising surgical margin rates, Eur. Urol. 80 (2) (2021) 213–221.
[24] M.S. Pollanen, DH. Ubelaker, Forensic significance of the polymorphism of hyoid bone shape, J. Forensic Sci. 42 (5) (1997) 890–892.
[25] DH. Ubelaker, Hyoid fracture and strangulation, J. Forensic Sci. 37 (5) (1992) 1216–1222.
[26] D. Gascho, J. Heimer, C. Tappero, S. Schaerli, Relevant findings on postmortem CT and postmortem MRI in hanging, ligature strangulation and manual strangulation and their additional value compared to autopsy - a systematic review, Forensic Sci. Med. Pathol. 15 (1) (2019) 84–92.
[27] H.M. de Bakker, P.C. Olsthoorn, V. Soerdjbalie-Makoe, BS. de Bakker, Comparison of post-mortem radiologic modalities to evaluate suspected neck violence, Forensic Imaging 21 (2020) 200373.
[28] K. Schulze, L.C. Ebert, T.D. Ruder, B. Fliss, S.A. Poschmann, D. Gascho, et al., The gas bubble sign-a reliable indicator of laryngeal fractures in hanging on post-mortem CT, Br. J. Radiol. 91 (1084) (2018) 20170479.
[29] M. Oehmichen, Vitality and time course of wounds, Forensic Sci. Int. 144 (2-3) (2004) 221–231.
[30] Z. Li, J.A. Clarke, R.A. Ketcham, M.W. Colbert, F. Yan, An investigation of the efficacy and mechanism of contrast-enhanced X-ray computed tomography utilizing iodine for large specimens through experimental and simulation approaches, BMC. Physiol. 15 (1) (2015) 1–16.
[31] S. Grabherr, J. Grimm, A. Dominguez, J. Vanhaebost, P. Mangin, Advances in post-mortem CT-angiography, Br. J. Radiol. 87 (1036) (2014) 20130488.
[32] K. Orhan, Micro-computed Tomography (micro-CT) in Medicine and Engineering, Springer, 2020.